

STATISTICAL MEASURES TO DESCRIBE THE VIBRATIONAL CHARACTERISTICS OF STRUCTURES WITH UNCERTAINTY

Geoff Lucas and Nicole Kessissoglou

School of Mechanical and Manufacturing Engineering

University of New South Wales (UNSW)

Sydney, NSW 2052, Australia

Predicting the vibro-acoustic responses of structures with uncertainty can be difficult. For example, the dynamic response of body panels in a vehicle can differ greatly across an ensemble of vehicles due to small variations in spot welds from the assembly process. In this paper, several statistical measures including the statistical overlap factor, distribution of modal spacings and an ergodic hypothesis are used to examine the natural frequencies and responses for a range of dynamic systems. Uncertainty across an ensemble of nominally identical structures has been generated by adding small masses and/or springs at random locations. A measure of the uncertainty is obtained by observing the variation in the natural frequencies of an ensemble member from their mean value across the ensemble. Using an ergodic hypothesis, a comparison between the mean vibrational response of an ensemble of nominally identical structures at each frequency is made with the frequency averaged response of a single ensemble member.

1. INTRODUCTION

For most practical engineering systems, there are degrees of uncertainty arising from variation in material properties, geometry and manufacturing tolerances [1]. Uncertainties are also observed in the variation in the natural frequencies and dynamic responses across an ensemble of nominally identical structures. For example, the interior noise levels have been measured for successive vehicles from a production line for which the frequency responses were found to differ by at least 10 dB [2,3]. The variation is in part attributed to the manufacturing and assembly process resulting in local material property changes. Furthermore, as the frequency increases, so does the sensitivity of dynamic responses to uncertainties.

A number of techniques have been developed to account for uncertainty in the dynamic models of structures; some are briefly mentioned in what follows. The stochastic finite element method using Monte-Carlo simulations can account for structural uncertainty [4,5], but this method is restricted by the amount of information required to model joints between subsystems [6] and the significant computational expense required. An improved finite element method which only uses the mean, variance and covariance of the properties of the uncertainty has been developed to reduce the computation time and increase accuracy of the results [7]. Perturbation methods based on the finite element method have also been used to investigate the dynamic response of structures with uncertain parameters [8]. Including the second and higher order terms in the perturbation analysis is sometimes necessary, however this increases the time required to obtain a solution. Interval analysis has been utilised to examine the effect of uncertainty in the material parameters and dimensions on the eigenvalues and dynamic responses of structures [9,10]. In this method,

the lower bound, upper bound and mean values of parameters with uncertainty were allowed to vary within a predefined band. A disadvantage of this method is that it produces very conservative results. A review of non-probabilistic approaches for uncertainty treatment in finite element analysis including both interval and fuzzy theory is given by Moens and Vandepitte [11].

In a pioneering paper, Weaver [12] transferred the study of the eigenvalues of random matrices in quantum mechanics to examine modal statistics in linear acoustics and vibrations. He showed that breaking physical symmetry by cutting slits into aluminium blocks results in the probability density function of the modal spacings being described by a Rayleigh distribution. These findings have been numerically and experimentally validated by examining the modal spacing distributions for vibrating plates with deformed boundaries [13] and for mass-loaded plates [14]. A motivation for this work is to investigate the modal spacing statistics of more complex structures which are a combination of both rigid body and flexural components, as well as structures coupled by joints with uncertain parameters.

In this paper, several statistical methodologies are used to investigate the natural frequencies and dynamic responses of structures with uncertainty across a wide frequency range. Attempting to predict and model all the various causes of uncertainty would be a very time consuming and difficult task. However, if the uncertainty becomes large enough, the response of a system becomes independent of the details of the uncertainty [1,15]. This paper attempts to address this statement by examining a range of dynamic systems corresponding to a mass-and-spring-loaded plate, two plates coupled by springs and a frame-plate structure. In each case, uncertainty is generated by adding point masses and/or springs at random

locations on the structures. A measure of the uncertainty across an ensemble of nominally identical structures is obtained using a non-dimensional parameter called the statistical overlap factor [16]. Statistical overlap occurs when there is sufficient random variation in an individual natural frequency of a system from its mean value across the ensemble. A measure of the uncertainty occurring in a single ensemble member is obtained by observing the distribution of the spacings between successive natural frequencies. A statistical measure of the dynamic response is examined using an ergodic hypothesis, in which the frequency averaged response of a single system in the ensemble is compared with the mean response averaged across the ensemble at each frequency.

2. STATISTICAL METHODOLOGIES

Modal spacing distributions

The earliest work on examining the distribution of the spacings between successive natural frequencies was conducted by Bolt [17] and Lyon [18]. They showed that for a perfectly rectangular room, the probability density function of the modal spacings followed an exponential distribution, which is given by

$$p(s) = ae^{-as}, \quad a = 1/\mu, \quad s \geq 0 \quad (1)$$

where μ is the mean spacing between neighbouring natural frequencies. However, later work has shown that an exponential distribution of the modal spacings only applies for simple and physically symmetrical structures and acoustic volumes such as a perfectly rectangular plate or box-shaped room. A Rayleigh distribution, which is given by [19]

$$p(s) = \frac{s}{c^2} e^{-s^2/2c^2}, \quad c = \mu\sqrt{2/\pi}, \quad s \geq 0 \quad (2)$$

of the modal spacings of a structure indicates that there is sufficient uncertainty in a structure such that its dynamic response is independent of the details of its uncertainty.

Statistical overlap factor

The statistical overlap factor is a useful parameter to obtain a measure of the amount of variation in the position of the modes across an ensemble of nominally identical systems with uncertainties and is defined by [16,20]

$$S = \frac{2\{\text{var}[\Delta\omega_n]\}^{1/2}}{\langle\omega_{n+1} - \omega_n\rangle} = \frac{2\sigma}{\mu} \quad (3)$$

where σ is the standard deviation of any particular natural frequency ω_n from its mean value due to uncertainties in the system and is measured across an ensemble of random structures. Statistical overlap occurs when the random variation in an individual natural frequency of a system exceeds the mean frequency spacing.

Ergodic hypothesis

The natural frequencies of structures with uncertainty can be considered to be ergodic in the sense that the statistical response of an ensemble are contained within one member of that ensemble [21]. Application of the ergodic hypothesis to

dynamic systems states that the mean response is ergodic such that the frequency averaged response is equal to the ensemble average and can be expressed by [20]

$$\langle e_i(\mathbf{x}, \omega, \mathbf{p}) \rangle_{\mathbf{p}} = \left(\frac{1}{\Delta\omega} \right) \int_{\Delta\omega} e_i(\mathbf{x}, \omega, \mathbf{p}) d\omega \quad (4)$$

where e_i is the kinetic energy density for subsystem i as a function of location \mathbf{x} and frequency ω . \mathbf{p} corresponds to a set of random parameters that describe the uncertainty in the system properties, $\langle \rangle_{\mathbf{p}}$ represents the ensemble average and $\Delta\omega$ is the frequency averaging bandwidth. The ergodic hypothesis requires the averaging bandwidth $\Delta\omega$ to be sufficiently wide such that frequency averaging the response of one member of the ensemble will be the same as averaging at a single frequency across the ensemble. A sufficiently wide averaging band would include at least 3 modes [20].

To implement the various aforementioned statistical methodologies, a range of dynamic systems are examined corresponding to a mass-and-spring-loaded plate, two plates coupled by springs and a frame-plate structure. In each case, uncertainty is generated by varying the location of the added masses and/or springs.

3. DYNAMIC MODELS OF STRUCTURES WITH UNCERTAINTY

Lagrange-Rayleigh-Ritz method

The equations of motion of a dynamic system in modal space can be derived using the Lagrange-Rayleigh-Ritz technique in what follows. The flexural displacement of a bare rectangular plate in modal space is given by [22]

$$w(x, y, t) = \sum_{mn} q_{mn}(t) \phi_{mn}(\mathbf{x}) \quad (5)$$

q_{mn} is the modal coordinate, and m, n are the mode numbers of the shape functions in the x and y directions respectively. $\phi_{mn}(\mathbf{x}) = \phi_m(x) \phi_n(y)$ are the mass-normalised eigenfunctions which satisfy the following orthogonality condition [23]

$$\int_0^{L_x} \int_0^{L_y} \rho h \phi_{mn} \phi_{m'n'} dx dy = \begin{cases} 1 & mn = m'n' \\ 0 & mn \neq m'n' \end{cases} \quad (6)$$

where L_x, L_y are respectively the lengths of the plate in the x and y directions, h is the plate thickness and ρ is the density. For a plate simply supported on all four sides, the mass-normalised eigenfunctions are given by

$$\phi_{mn} = \frac{1}{M_n} \sin\left(\frac{m\pi x}{L_x}\right) \sin\left(\frac{n\pi y}{L_y}\right) \quad (7)$$

where $M_n = \rho h L_x L_y / 4$ is the modal mass. Using the orthogonality condition, an expression for the kinetic energy of a bare plate becomes

$$\begin{aligned} T &= \frac{\rho h}{2} \int_0^{L_x} \int_0^{L_y} \dot{w}^2(\mathbf{x}) dx dy = \frac{\rho h}{2} \sum_{mn} \sum_{jk} \dot{q}_{mn} \dot{q}_{jk} \phi_{mn}(\mathbf{x}) \phi_{jk}(\mathbf{x}) \\ &= \frac{1}{2} \sum_{mn} \dot{q}_{mn}^2 \end{aligned} \quad (8)$$

where \dot{w} denotes the derivative of w with respect to time. Similarly, an expression for the potential energy of the plate can be obtained as

$$V = \frac{1}{2} \sum_{mn} \omega_{mn}^2 q_{mn}^2 \quad (9)$$

where $\omega_{mn} = \sqrt{\frac{D}{\rho h} \left(\left(\frac{m\pi}{L_x} \right)^2 + \left(\frac{n\pi}{L_y} \right)^2 \right)}$ corresponds to

the natural frequencies of the bare plate,

$$D = \frac{Eh^3}{12(1-\nu^2)}$$

is the plate flexural rigidity, and E, ν are

respectively Young's modulus and Poisson's ratio.

Lagrange's equation for a particular modal coordinate j is given by [22]

$$\frac{d}{dt} \left(\frac{\partial T}{\partial \dot{q}_j} \right) - \frac{\partial T}{\partial q_j} + \frac{\partial V}{\partial q_j} = 0, \quad j = 1, 2, \dots, N \quad (10)$$

Differentiating the kinetic and potential energies given by Eqs. (8) and (9) with respect to the modal coordinate pq and substituting into Lagrange's equation results in the equation of motion of the bare plate.

$$\ddot{q}_{pq} + \omega_{pq}^2 q_{pq} = 0 \quad (11)$$

The natural frequencies can then be obtained by eigenvalue analysis $(\mathbf{K} - \omega^2 \mathbf{M})\mathbf{p} = 0$. This was performed in Matlab using the command *eig*, which returns a diagonal matrix of eigenvalues and a matrix of corresponding eigenvectors.

Mass-and-spring-loaded plate

Now consider a mass-and-spring-loaded plate as shown in Fig. 1. For the simply supported plate in free vibration with N_m number of point masses (of size m) and N_k springs to ground (of stiffness k), the equation of motion for a particular modal coordinate pq of the bare plate has been previously developed and is given by [24]

$$\ddot{q}_{pq} + \sum_{mn} \sum_{N_m} m \ddot{\phi}_{mn} \phi_{mn}(\mathbf{x}_m) \phi_{pq}(\mathbf{x}_m) + \sum_{mn} \sum_{N_k} k q_{mn} \phi_{mn}(\mathbf{x}_k) \phi_{pq}(\mathbf{x}_k) + \omega_{pq}^2 q_{pq} = 0 \quad (12)$$

\mathbf{x}_m and \mathbf{x}_k correspond to the random locations of the added masses and springs, respectively. In the absence of the added masses and springs, Eq. (12) simply reduces to that of the bare plate given by Eq. (11). The natural frequencies of the mass-spring loaded plate were obtained by eigenvalue analysis using Matlab.

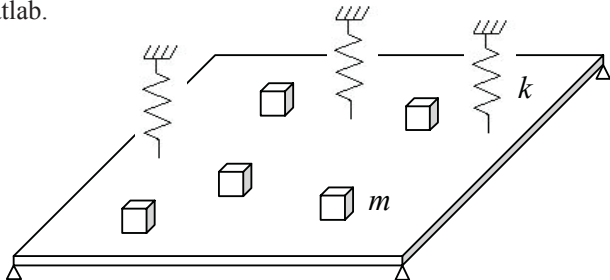


Figure 1. A simply supported plate with randomly located point masses and springs to ground.

Plates coupled by springs

Consider two simply supported plates coupled by a linear spring of stiffness k at a random location \mathbf{x}_1 on each plate ($i=1,2$ is the plate number). The total kinetic energy of the system is

$$T = \frac{\rho_1 h_1}{2} \int_0^{L_{x1}} \int_0^{L_{y1}} \dot{w}_1^2(\mathbf{x}) dx dy + \frac{\rho_2 h_2}{2} \int_0^{L_{x2}} \int_0^{L_{y2}} \dot{w}_2^2(\mathbf{x}) dx dy = \frac{1}{2} \sum_{mn} \dot{q}_{1,mn}^2 + \frac{1}{2} \sum_{mn} \dot{q}_{2,mn}^2 \quad (13)$$

Making use of the eigenfunction orthogonality conditions, the potential energy of the coupled plate system is given by

$$V = \frac{1}{2} \sum_{mn} \omega_{1,mn}^2 q_{1,mn}^2 + \frac{1}{2} \sum_{mn} \omega_{2,mn}^2 q_{2,mn}^2 + \frac{k}{2} (w_1(\mathbf{x}_1) - w_2(\mathbf{x}_2))^2 \quad (14)$$

where $\omega_{1,mn}$ and $\omega_{2,mn}$ are the natural frequencies of each uncoupled plate. The last term on the right hand side of Eq. (14) describes the coupling dynamics due to the randomly located spring. Differentiating the kinetic and potential energies with respect to the modal coordinate pq of the uncoupled plates and substituting into Lagrange's equation, the equations of motion for the spring-coupled plates are given by

$$\ddot{q}_{1,pq} + k \phi_{1,pq}(\mathbf{x}_1) \sum_{mn} q_{1,mn} \phi_{1,mn}(\mathbf{x}_1) - k \phi_{1,pq}(\mathbf{x}_1) \sum_{jk} q_{2,jk} \phi_{2,jk}(\mathbf{x}_2) + \omega_{1,pq}^2 q_{1,pq} = 0 \quad (15)$$

$$\ddot{q}_{2,pq} + k \phi_{2,pq}(\mathbf{x}_2) \sum_{jk} q_{2,jk} \phi_{2,jk}(\mathbf{x}_2) - k \phi_{2,pq}(\mathbf{x}_2) \sum_{mn} q_{1,mn} \phi_{1,mn}(\mathbf{x}_1) + \omega_{2,pq}^2 q_{2,pq} = 0 \quad (16)$$

Equations (15) and (16) can easily be expanded to account for N number of randomly located springs, as shown in Fig. 2. The natural frequencies of the spring-coupled plates were obtained by eigenvalue analysis using Matlab.

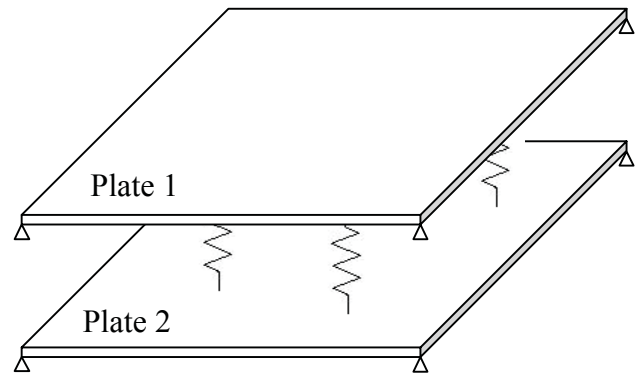


Figure 2. Simply supported plates coupled by randomly located springs.

Frame-plate structure

Finally, it is of interest to examine the dynamic characteristics of a structure with both stiff and flexible components, where the dynamic responses of the stiff components (of low modal density) are not sensitive to uncertainties but the flexible components (of high modal density) are sensitive to uncertainties. The dynamic characteristics of a frame-plate structure were obtained both

computationally and experimentally. The frame-plate structure was modelled using finite element analysis, where the flexible plates were represented by quad 4 elements and the frame was modelled using bar elements. Damping was included in the model using a structural loss factor of 0.1%. The frame was constructed from 19 mm square hollow section aluminium tubes with a wall thickness of 1.2 mm. The flexible plates were made from 1.6 mm thick aluminium plate. The overall dimensions of the structure were 1000 mm long, 600 mm high and 600 mm wide. Twenty 3 gram masses were attached to the structure (7 masses on the two side plates and 6 masses on the base plate). Using Monte-Carlo simulations, 50 different configurations of the randomly located masses have been solved. Figure 3 shows a computational model of an ensemble member of the frame-plate structure.

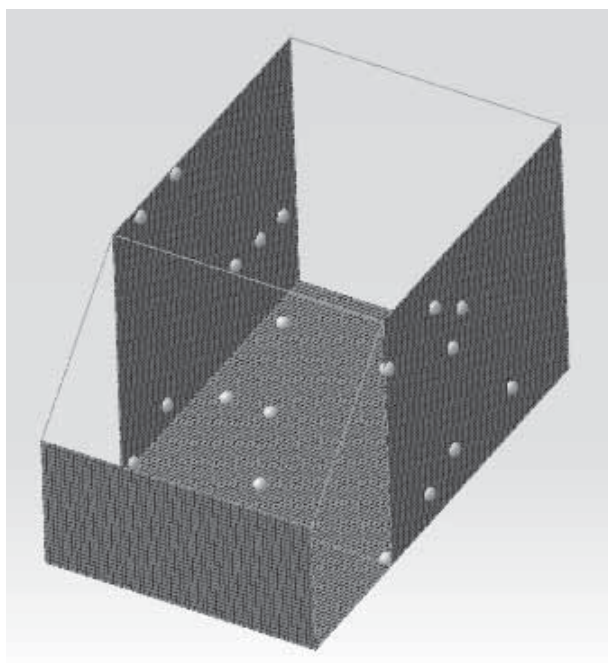


Figure 3. FEA model of the frame-plate structure with randomly located masses attached to the plates.

The same dimensions and material parameters were used in the construction of the experimental rig of the frame-plate structure. The tubes for the frame were welded together and the plates were attached using an epoxy adhesive. The frame was hung on soft springs to simulate free-free boundary conditions. Twenty 3 gram masses were attached at random locations across three of the plates. The structure was excited by a shaker mounted horizontally to the front, lower left hand corner of the frame, as shown in Fig. 4. The responses were measured in the horizontal plane at the rear, top, right hand corner. The measured signals from both the excitation and the response were passed through charge conditioning amplifiers before being sampled by an FFT analyser. 50 different configurations have been measured by randomising the locations of the added masses.

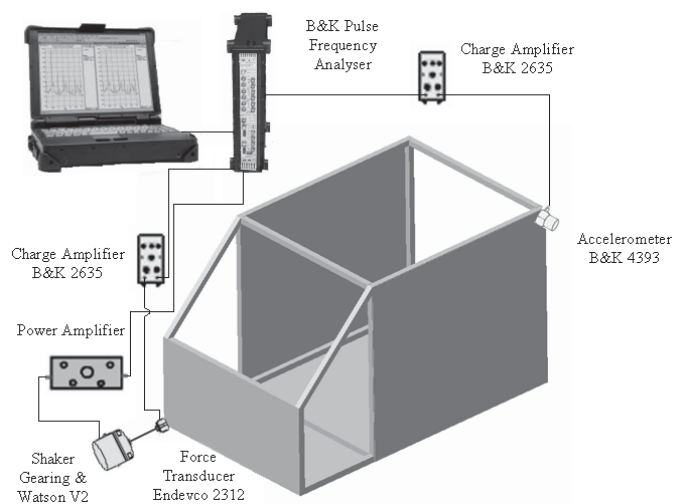


Figure 4. Schematic diagram of the experimental set-up for the frame-plate structure.

4. RESULTS

Natural frequency statistics

The natural frequencies for the bare plate, mass-and-spring-loaded plate and plates coupled by linear springs were obtained using Matlab. In each case, the plates were of dimensions $L_x=899$ mm, $L_y=600$ mm and thickness $h=2$ mm, with material properties of aluminium ($\rho=2800$ kg/m³, $E=70$ GPa, $\nu=0.3$). Damping was included in the analysis by using a complex Young's modulus $E(1+j\eta)$ where $\eta=0.1\%$ is the structural loss factor. A probability density function (PDF) of the modal spacings was achieved by conducting the following steps: the natural frequencies for each dynamic system were arranged in ascending order, the spacings between successive frequencies were obtained, a histogram of the frequency spacings was generated and then converted to a PDF by scaling to unit area. The mean frequency spacing for each ensemble member was also calculated for comparison of the PDFs with the Rayleigh and exponential distributions. It is worth noting that the mean frequency spacing for a given dynamic system does not significantly vary between each ensemble member.

Figure 5 presents the frequency spacing distribution of the bare plate. The frequency spacings were obtained for a frequency range up to 4 kHz and the mean frequency spacing is approximately 12 Hz. Figure 5 shows that the modal spacing distribution of a structure with physical symmetries clearly follows an exponential distribution, which is given by Eq. (1) and is a function of the mean frequency spacing of the bare plate.

The PDF of the modal spacings and statistical overlap factor results for the mass-and-spring-loaded plate are given by Figs. 6 and 7. Fifty masses and springs were added at random locations, where each mass represents 0.2% of the mass of the bare plate and the springs each have stiffness 2×10^5 N/m. The added masses and springs were considered to be both non-collocated (Fig. 6) and collocated (Fig. 7). Using Eq. (3), the statistical overlap factor (SOF) was calculated by examining

the variation of each natural frequency across an ensemble of 50 spring-mass plates. The trend line for the SOF curves is also shown. The curves of the statistical overlap factor tend to level off with increasing frequency. This indicates that the results for the SOF have ‘saturated’ such that no further increase in statistical overlap will be observed with increasing frequency. The saturation in the SOF is attributed to the fact that the dynamic characteristics of the system have become independent of the details of the uncertainty, thereby indicating the frequency range beyond which a Rayleigh distribution of the modal spacings is expected to apply. An interesting observation in Fig. 7 for the plate ensemble with collocated masses and springs is the distinct dip in the statistical overlap factor, at which the value for S is zero. The frequency at which this dip occurs corresponds to the natural frequency for an equivalent single degree of freedom spring-mass system in terms of the added masses and springs, that is, $\omega_n = \sqrt{kN_k / mN_m}$ (which in this case occurs at approximately 916 Hz). At this frequency, the impedance of the added masses and springs is zero and hence are not generating any uncertainty on the plate. The low frequency range corresponds to the stiffness controlled region in which the springs dominate the structural response. As the frequency increases, the dynamic response of the structure becomes more sensitive to the inertial effects of the added point masses. The PDFs were obtained for the modal ranges beyond which the SOF begins to level off (4 kHz to 12 kHz). For both the collocated and non-collocated masses and springs, the PDF of the modal spacings clearly follows a Rayleigh distribution, which was calculated using Eq. (2) and the mean frequency spacing of an ensemble member for the same frequency range.

A PDF of the frequency spacings (for a single ensemble member) and statistical overlap factor (for the ensemble) are given in Figs. 8 and 9 for the spring-coupled plates and frame-plate structure respectively. For the spring-coupled plates, 10 springs of linear stiffness 5e6 N/m were randomly located on each plate. Similar results are observed for each system where the SOF initially increases with increasing frequency and then tends to level off as the statistical overlap saturates. The PDFs of the modal spacings are given for the frequency ranges 2 kHz to 10 kHz (spring-coupled plates) and 1 kHz to 4 kHz (frame-plate structure).

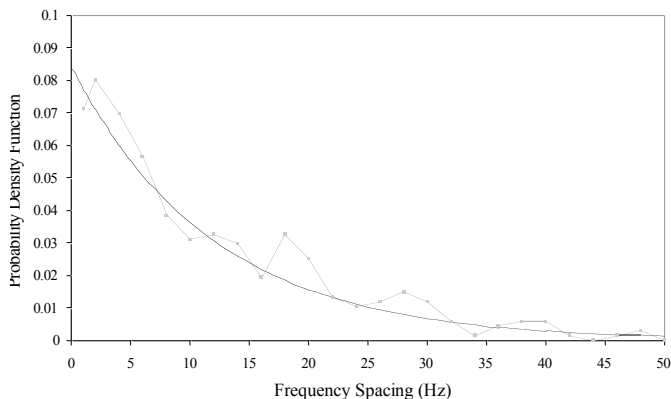


Figure 5. Probability density function of the natural frequency spacings for the bare plate: simulation results (grey line); exponential distribution (black line).

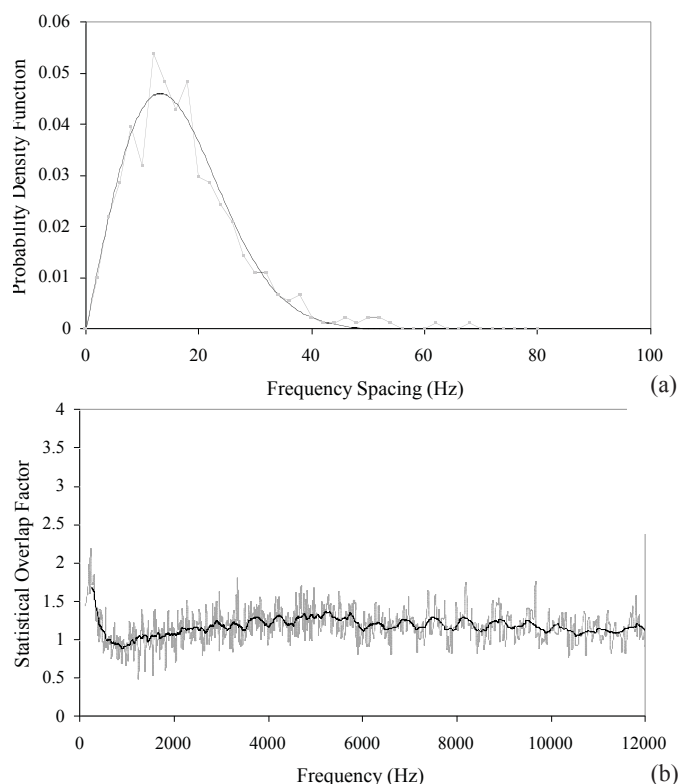


Figure 6. Results for the mass-and-spring-loaded plate (non-collocated masses and springs). (a) Probability density function of the modal spacings: simulation results (grey line); Rayleigh distribution (black line). (b) Statistical overlap factor (grey line) and trend curve (black line).

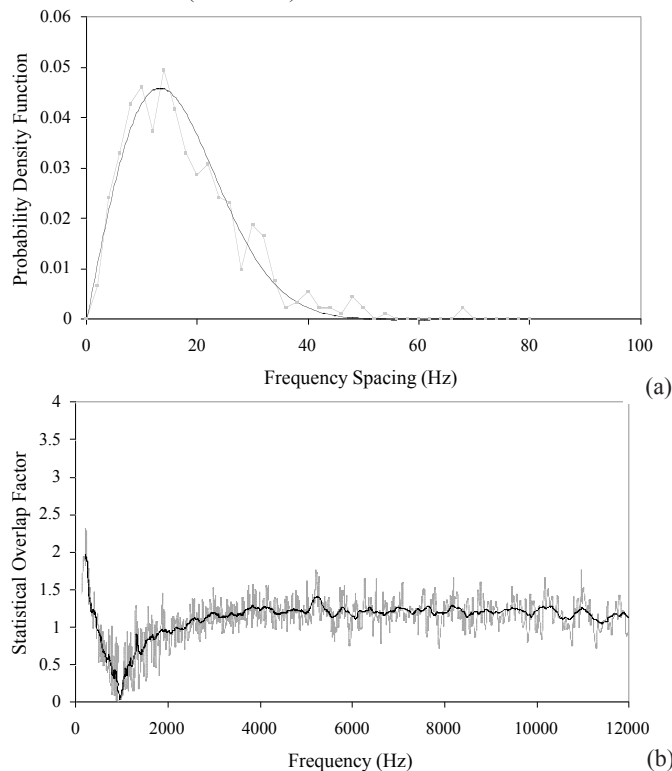
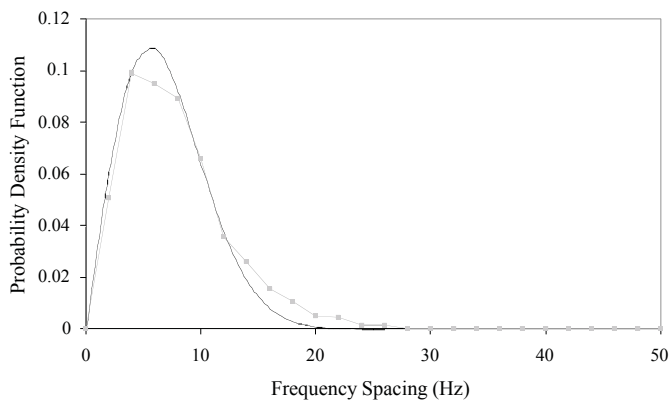
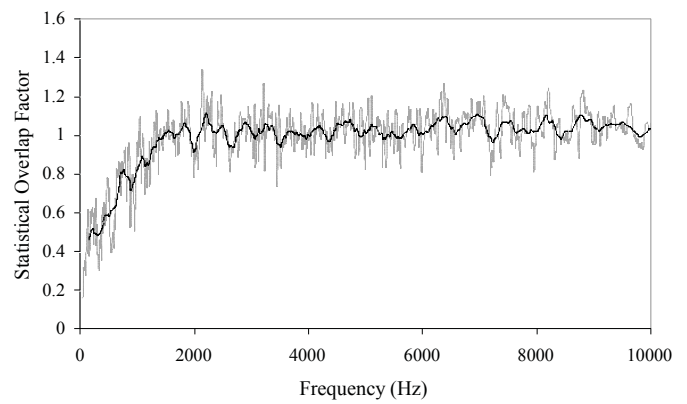


Figure 7. Results for the mass-and-spring-loaded plate (collocated masses and springs). (a) Probability density function of the modal spacings: simulation results (grey line); Rayleigh distribution (black line). (b) Statistical overlap factor (grey line) and trend curve (black line).

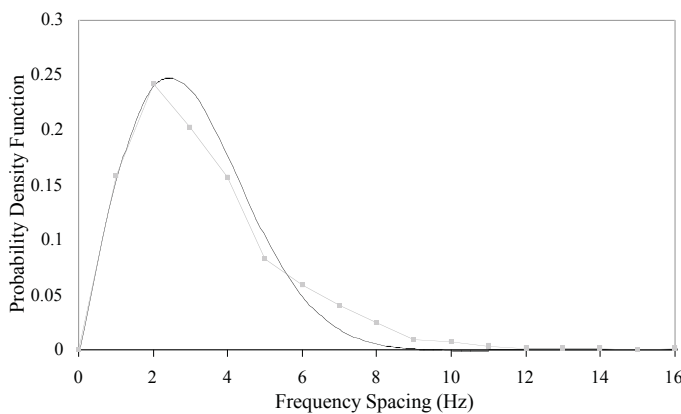


(a)

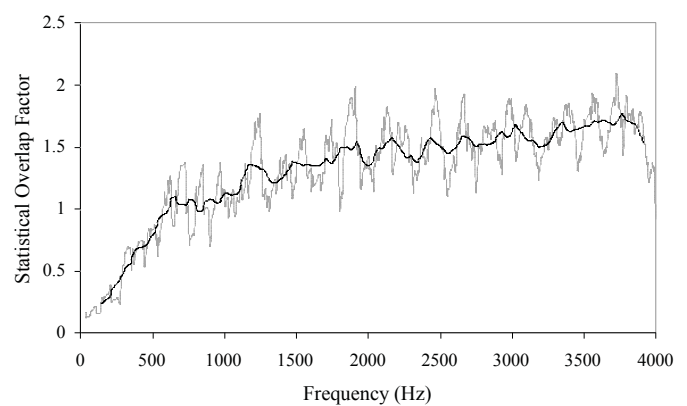


(b)

Figure 8. Results for the spring-coupled plates. (a) Probability density function of the modal spacings: simulation results (grey line); Rayleigh distribution (black line). (b) Statistical overlap factor (grey line) and trend curve (black line).



(a)



(b)

Figure 9. Results for the frame-plate structure. (a) Probability density function of the modal spacings: simulation results (grey line); Rayleigh distribution (black line). (b) Statistical overlap factor (grey line) and trend curve (black line).

Frequency and ensemble averaged responses

In this section, the ergodic hypothesis has been utilised to compare the frequency averaged and ensemble averaged responses for the spring-coupled plates and the frame-plate structure. The frequency averaged response of a single ensemble member was obtained by averaging the response using a proportional bandwidth of 5% of the frequency range for the spring-coupled plates, and 2% of the frequency range for the frame-plate structure. The ensemble averaging was achieved by averaging the responses across the ensemble at each discrete frequency. A measure of the quality of the match between the ensemble and frequency averaged results is observed using the z-score, which tests whether the residuals (corresponding to the error between the frequency and ensemble averaged results) has a mean of zero. The z-score is given by $z=x/\sigma_r$, where x is the mean of the residuals and σ_r is the standard deviation of the residuals.

The frequency and ensemble averaged energy levels of the spring-coupled plates are shown in Fig. 10. Very good agreement

between the ensemble averaged and frequency averaged results is observed. The corresponding z-score is calculated to be $|z|=0.0091$ with a standard deviation of the residuals, $\sigma_r = 4$ dB. Similarly, Figs. 11 and 12 present the frequency averaged and ensemble averaged responses for the frame-plate structure obtained computationally (Fig. 11) and experimentally (Fig. 12). The z-scores are $|z|=0.0668$ and $\sigma_r = 3.2$ dB (computational result) and $|z|=0.0343$, $\sigma_r = 5.2$ dB (experimental result). In order to observe the effect of the frequency averaging bandwidth on the ergodic hypothesis results, the z-score and standard deviation for a range of averaging bandwidths are presented in Table 1, for the spring-coupled plates and frame-plate structure. It can be seen that increasing the averaging bandwidth results in a decrease in the z-score and standard deviation and hence an increase in the similarity between the ensemble and frequency averaged results. This decrease in the z-score and standard deviation will occur until an optimum frequency averaging bandwidth is reached. Beyond this bandwidth, the z-score and standard

deviation will increase again due to loss of detail in the responses. The ergodic hypothesis shows the potential of obtaining the statistical responses of an ensemble of nominally identical structures from just one member of the ensemble.

Table 1. The z-score and standard deviations for a range of frequency averaging bandwidths for the spring-coupled plates and frame-plate structure.

Spring-coupled plates

Bandwidth (%)	1	2	3	4	5	10
z-score	0.2730	0.1799	0.1071	0.0515	0.0091	0.1215
Std deviation	6.6070	5.3469	4.5975	4.1723	3.9827	3.9211

Frame-plate structure (computational results)

Bandwidth (%)	0.1	0.25	0.5	1	2	5
z-score	0.2129	0.1769	0.0934	0.0668	0.2142	0.3361
Std deviation	4.4364	3.9901	3.4342	3.1548	3.7253	4.7828

Frame-plate structure (experimental results)

Bandwidth (%)	0.1	0.25	0.5	1	2	5
z-score	0.1763	0.1544	0.1112	0.0343	0.0631	0.1807
Std deviation	6.1878	5.9180	5.5609	5.2406	5.3509	6.0253

5. CONCLUSIONS

The statistical responses of a mass-and-spring-loaded plate, two plates coupled by springs and a frame-plate structure have been investigated. For complex structures, it was found that the spacings between successive natural frequencies of a structure follow a Rayleigh distribution, indicating that the response of the structure is independent of the properties of the uncertainty. An ergodic hypothesis was employed which showed that the statistical responses of an ensemble can be predicted by frequency averaging the response of one member of the ensemble, as long as the averaging bandwidth is sufficiently wide. The results presented in this paper demonstrate that there are universal statistical descriptors for the modal spacings and dynamic responses of structures with sufficient uncertainty. This can serve to reduce the computational difficulties involved in the study of complex systems.

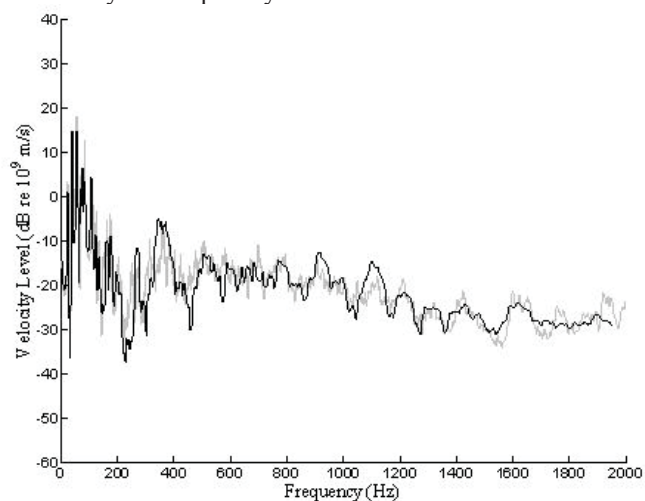


Figure 10. The frequency averaged response (black line) and ensemble averaged response (grey line) for the spring-coupled plates.

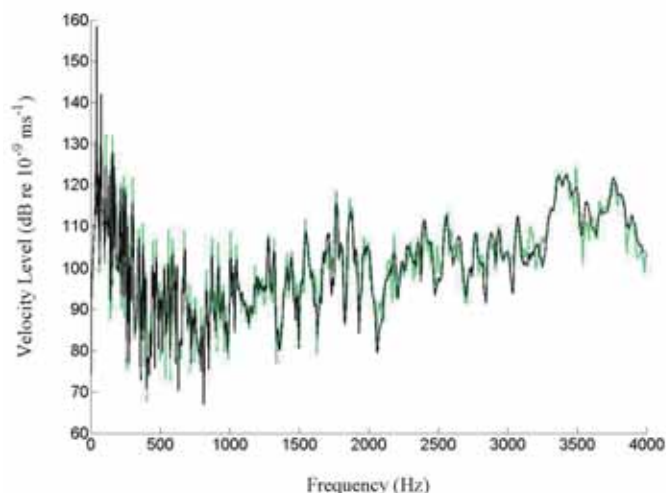


Figure 11. The frequency averaged response (black line) and ensemble averaged response (grey line) for the frame-plate structure (computational result).

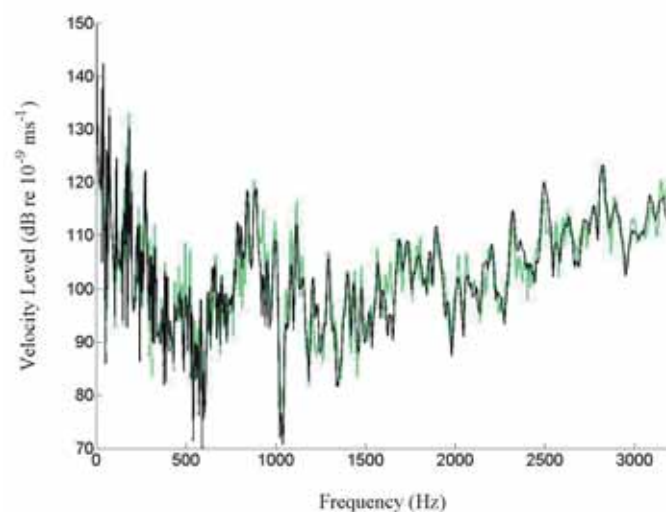


Figure 12. The frequency averaged response (black line) and ensemble averaged response (grey line) for the frame-plate structure (experimental result).

REFERENCES

- [1] R.S. Langley, "Mid and high-frequency vibration analysis of structures with uncertain properties", *Proceedings of the Eleventh International Conference on Sound and Vibration*, St. Petersburg, Russia, 5-8 July 2004.
- [2] R. Cornish, "A novel approach to optimizing and stabilising interior noise quality in vehicles", *Proceedings of the Institute of Mechanical Engineers, Part D - Journal of Automobile Engineering* **7** (214), 685-692 (2000).
- [3] M.S. Kompella and R.J. Bernhard, "Variation of structural-acoustic characteristics of automotive vehicles", *Noise Control Engineering Journal* **44**, 93-99 (1996).
- [4] M. Kleiber and T.D. Hein, *The Stochastic Finite Element Method*, John Wiley and Sons, 1992.
- [5] M. Papadrakakis and A. Kotsopoulos, "Parallel solution methods for stochastic finite element analysis using Monte Carlo simulation", *Computer Methods in Applied Mechanics and Engineering* **168**, 305-320 (1999).

- [6] P.J. Shorter, "A review of mid-frequency methods for automotive structure-borne noise", *SEA International Noise and Vibration Conference and Exhibition*, Traverse City, Michigan, May 5-8 2003.
- [7] G. Stefanou and M. Papadrakakis, "Stochastic finite element analysis of shells with combined random material and geometric properties", *Computer Methods in Applied Mechanics and Engineering* **193**, 139-160 (2004).
- [8] M. Kaminski, "Perturbation based on stochastic finite element method homogenization of two-phase elastic composites", *Computers and Structures* **78**, 811-826 (2000).
- [9] S.H. Chen, H.D. Lian and X.W. Yang, "Interval eigen analysis for structures with interval parameters", *Finite Elements in Analysis and Design* **39**, 419-431 (2003).
- [10] Z. Qui and X. Wang, "Parameter perturbation method for dynamic responses of structures with uncertain-but-bounded parameters based on interval analysis", *International Journal of Solids and Structures* **42**, 4958-4970 (2005).
- [11] D. Moens and D. Vandepitte, "A survey of non-probabilistic uncertainty treatment in finite element analysis", *Computer Methods in Applied Mechanics and Engineering* **194**, 1527-1555 (2005).
- [12] R.L. Weaver, "Spectral statistics in elastodynamics", *Journal of the Acoustical Society of America* **85**, 1005-1013 (1989).
- [13] P. Bertelsen, C. Ellegaard and E. Hugues, "Distribution of eigenfrequencies for vibrating plates", *European Physical Journal B* **15**, 87-96 (2000).
- [14] R.S. Langley and A.W.M. Brown, "The ensemble statistics of the energy of a random system subjected to harmonic excitation", *Journal of Sound and Vibration* **275**, 823-846 (2004).
- [15] R.H. Lyon and R.G. DeJong, *Theory and Application of Statistical Energy Analysis*, 2nd ed. Butterworth Heinemann, Oxford, 1995.
- [16] C.S. Manohar and A.J. Keane, "Statistics of energy flows in spring-coupled one-dimensional subsystems", *Philosophical Transactions: Physical Sciences and Engineering* **346**, 525-542 (1994).
- [17] R.H. Bolt, "Normal frequency spacing statistics", *Journal of the Acoustical Society of America* **19**, 79-90 (1947).
- [18] R.H. Lyon, "Statistical analysis of power injection and response in structures and rooms", *Journal of the Acoustical Society of America* **45**, 545-565 (1969).
- [19] M.L. Mehta, *Random Matrices*, 3rd ed. Elsevier Academic Press, 2004.
- [20] R.S. Langley, "SEA: current and future research needs", *Proceedings of the First International AutoSEA Users Conference*, Westin/Sheraton Harbour Island, San Diego, CA, 27-28 July 2000.
- [21] A. Pandey, "Statistical properties of many-particle spectra III. Ergodic behavior in random-matrix ensembles", *Annals of Physics* **119**, 170-191 (1979).
- [22] L. Meirovitch, *Elements of vibration analysis*, 2nd ed. McGraw Hill, New York, 1986.
- [23] S. Timoshenko and S. Woinowsky-Krieger, *Theory of Plates and Shells*, McGraw-Hill, Singapore, 1959.
- [24] N.J. Kessissoglou and R.S. Langley, "Natural frequency statistics of engineering structures", *Proceedings of the Eleventh International Congress on Sound and Vibration*, St. Petersburg, Russia, 5-8 July 2004.

ARL

Sales & Hire

RION

Noise, Vibration & Weather Loggers

Sound & Vibration Measuring Instruments

EL-316 Type1 Noise Logger
 Sound Level Meters
 Entertainment Noise Monitors
 Vibration Equipment



Rion's NEW NA-28

- Easy to use compact design with comprehensive features
- Complies with IEC 61072-1:2002 & IEC 61260:1995
- Real Time Octaves & 1/3 Octaves
- Data stored as text files direct to CF Card

Acoustic Research Laboratories

Proprietary Limited

A.B.N. 47 050 100 804

Noise and Vibration Monitoring Instrumentation for Industry and the Environment

www.acousticresearch.com.au



ARL Sydney: (02) 9484-0800 Wavecom Melbourne: (03) 9897-4711

Instru-Labs Perth: (08) 9356 7999 Wavecom Adelaide: (08) 8331-8892 Belcur Brisbane: (07) 3820 2488